HEFAT2011
8th International Conference on Heat Transfer, Fluid Mechanics and Thermodynamics
11 – 13 July 2011
Pointe Aux Piments, Mauritius

HEAT REJECTION IN CONDENSERS CLOSE TO CRITICAL POINT - DESUPERHEATING, CONDENSATION IN SUPERHEATED REGION AND CONDENSATION OF TWO PHASE FLUID -

Hrnjak P.S.*[a,b] and Kondou Chieko[a]
*Author for correspondence

[a] Department of Mechanical Science and Engineering,
University of Illinois at Urbana-Champaign,
Urbana, IL 61801,USA, pega@illinois.edu

[b] Creative Thermal Solutions, Inc.
Urbana IL, 61802, USA,
pega@creativethermalsolutions.com

ABSTRACT

Conventional modeling of condensers always assumes three zones: desuperheating, condensation and subcooling even it is clear that condensation occurs in desuperheating zone at some conditions and that subcooling occurs during condensation. This paper discusses the actual situation and provides experimental validation of the hypothesis. The experimental results show heat transfer coefficients (HTC) of CO_2 and R410A at mass fluxes 100 to 240 kg $m^{-2}s^{-1}$ and reduced pressures from 0.68 to 1.00 in a horizontal smooth tube of 6.1 mm inner diameter. Data are compared to correlations proposed for other working fluids or other conditions. Results show much higher values of HTC than correlation proposed for single-phase turbulent flow in superheated zone. The occurrence of condensation in superheat zone is evident when tube wall temperature is below saturation temperature. The results suggest that simplified calculations of heat rejection in superheated zone significantly oversize the condenser. The semi-empirical correlation, which is here proposed as the combination of existing correlations for single-phase turbulent and saturated condensation, satisfactorily predicts the heat transfer coefficient of the superheat zone condensation.

INTRODUCTION

Balekjian and Katz [1] experimentally investigated condensation from superheated vapors of R114 and steam on outer surface of a horizontal tube. Their experimental HTC suggested the lowering cooling surface temperature, below saturation point, generates condensate from super heated vapor. Altman et al. [2] provided six points of experimentally determined HTC, which are averaged from various superheated inlet to saturated outlet in a test section of 1.22 m length 8.71 mm ID. With those six data having various superheat degree at test section inlet, approximately 30 to 70 % decrease in HTC from a correlation valid for two-phase zone condensation was confirmed. Bell [3] accepted the criterion of condensation occurrence in desuperheating zone is the tube wall temperature below saturation point and cautioned that the simple use of LMTD method to calculate the overall coefficient of condensers could be invalid. Miropolskiy et al. [4] provided experimental data for the quasi-local HTC of superheated steam vapor flowing downward in a cooled vertical smooth tube. The results experimentally presented the criterion of start of condensation which is when the tube wall temperature is below saturation point. Further, their data showed the behavior of superheat zone condensation for various reduced pressure until 0.82. Fujii et al. [5] experimentally investigated condensation of R11 and R113 flow in horizontal smooth tubes. From the temperature distribution in the radial direction of the horizontal middle plane of the tube, they proved coexistence of superheated vapor and subcooled liquid in condensation flow. They varied the vapor mass quality, which indicates actual vapor and liquid mass flow rate in non-equilibrium, to analyze the mass transport process. Lee et al. [6] experimentally investigated condensation in superheated R22 vapor and proposed a physical model accounting the sensible heat on the condensation heat transfer. Their model defines HTC bulk temperature as the reference temperature. In response, Webb [7] reported that sensible heat is negligible and simplified model defines HTC with saturation temperature gives same results to Lee's model.

Various systems and application drove operating conditions closer to the critical point, very often rejected heat in superheat zone is greater than in two-phase zone. Conditions just below the critical point are increasingly common for both R410A water heaters and CO_2 commercial refrigeration systems in most frequent operations from autumn to spring. The authors [8] presented experimental results for only CO_2 heat rejection (cooling/condensation) flow in 6.1 mm ID smooth tube at the pressure from 5.0 to 7.5MPa. The experimental results

identified the condensation in superheated vapor. In order to strengthen experimental verification one additional refrigerant R410A was explored. It was chosen because of its importance in applications and the effect of the refrigerant properties on condensation heat transfer.

NOMENCLATURE

P	pressure	[Pa]
T	temperature	[°C]
h	specific enthalpy	[J kg^{-1}]
x_b	thermodynamic vapor quality	[-]
q	heat flux	[W m^{-2}]
$\dot{Q}$	heat transfer rate	[W]
ΔZ_α	active cooling length of test tube	[m]
$\dot{m}$	mass flow rate	[kg s^{-1}]
G	mass flux	[kg m^{-2}s^{-1}]
d_i	inner diameter of test tube	[m]
Δh_{LV}	latent heat	[J kg^{-1}]
Cp	isobaric heat capacity	[J kg^{-1}K^{-1}]
g	gravitational acceleration	[m s^{-2}]
f	Darcy-Weisbach friction factor	[-]
F_a	correction factor for radial property change	[-]
J	dimensionless vapor velocity	[-]
Nu	Nusselt number	[-]
Pr	Prandtl number	[-]
HTC	See α	

Greek symbols

α	heat transfer coefficient (same as HTC)	[W m^{-2}K^{-1}]
ρ	density	[kg m^{-3}]
μ	viscosity	[Pa·s]
λ	thermal conductivity	[W m^{-1}K^{-1}]
X_{tt}	Lockhart–Martinelli parameter for turbulent $= (1/x_b - 1)^{0.9}(\rho_{Vsat}/\rho_{Lsat})^{0.5}(\mu_{Lsat}/\mu_{Vsat})^{0.1}$	[-]

Subscripts

i	inlet
o	outlet
MC	mixing chamber
PC	pre-cooler
TS	test section
V	vapor
L	liquid
r	refrigerant
H2O	water
wi	interior tube wall or evaluated at interior tube wall temperature
b	evaluated at bulk temperature
f	evaluated at film temperature
sat	evaluated at saturation temperature
SH	superheat
SC	subcool
latent	latent heat
gain	heat gain from ambient air through insulations
cond	conduction heat from our of active cooling length

CONDENSING SUPERHEAT ZONE

Figure 1 illustrates the heat flow and the temperature profile in condensing superheat zone, where bulk mean refrigerant temperature is above saturation point. According to Soliman's flow regime [9], condensation begins as mist flow and then changes into annular flow. According to Altman [2], thin ridges or droplets flow on the interior tube surface. Figure 1 explains the heat exchange with annular flow model for simplification.

From continuity, the total mass flow rate $\dot{m}_{total}$ of vapor and liquid refrigerant is,

$$\dot{m}_{total} = \dot{m}_{V,i} + \dot{m}_{L,i} = \dot{m}_{V,o} + \dot{m}_{L,o} \tag{1}$$

The amount of condensate $\Delta\dot{m}_L$ generated through a segment is expressed from the continuity as,

$$\Delta\dot{m}_L = \dot{m}_{L,o} - \dot{m}_{L,i} = \dot{m}_{V,i} - \dot{m}_{V,o} = \Delta\dot{m}_V \tag{2}$$

The average enthalpies in superheated vapor and subcooled liquid are represented with heat capacities and degree of superheat and subcool ΔT_{SH} ΔT_{SC} as,

$$\begin{aligned} \bar{h}_V &= h_{Vsat} + \overline{Cp_V \Delta T_{SH}} = h_{Vsat} + \overline{\Delta h_{SH}} \\ \bar{h}_L &= h_{Lsat} - \overline{Cp_L \Delta T_{SC}} = h_{Vsat} - \Delta h_{LV} - \overline{\Delta h_{SC}} \end{aligned} \tag{3}$$

Total inlet heat at the entrance of a segment is,

$$\begin{aligned} h_{b,i}\dot{m}_{total} &= \bar{h}_{V,i}\dot{m}_{V,i} + \bar{h}_{L,i}\dot{m}_{L,i} \\ &= \left(h_{Vsat} + \overline{\Delta h_{SH,i}}\right)\dot{m}_{V,i} + \left(h_{Vsat} - \Delta h_{LV} - \overline{\Delta h_{SC,i}}\right)\dot{m}_{L,i} \end{aligned} \tag{4}$$

Similarly, the total outlet heat at the exit of a segment is,

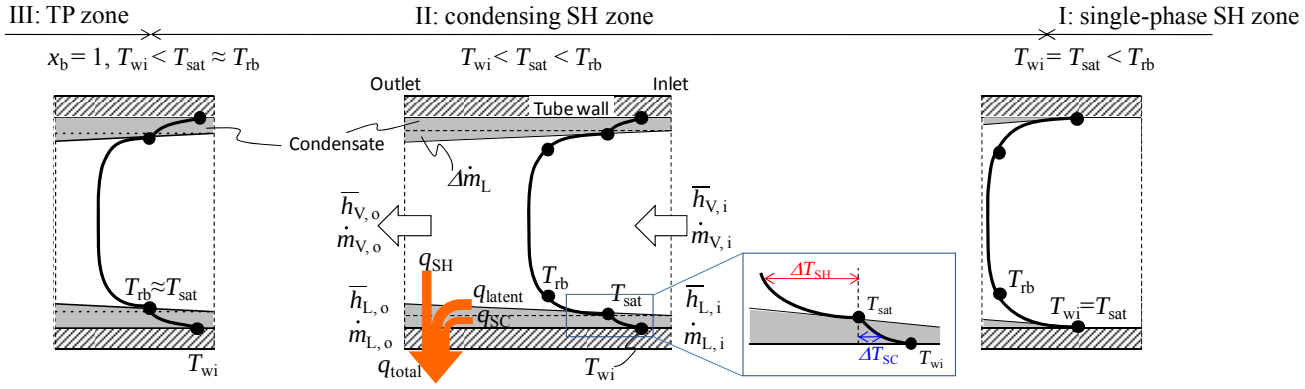

Figure 1 Illustration of heat flow and temperature distribution in the condensing superheat zone

$$h_{\mathrm{b,o}}\dot{m}_{\mathrm{total}} = \overline{h}_{\mathrm{V,o}}\dot{m}_{\mathrm{V,o}} + \overline{h}_{\mathrm{L,o}}\dot{m}_{\mathrm{L,o}}$$
$$= \left(h_{\mathrm{Vsat}} + \overline{\Delta h_{\mathrm{SH,o}}}\right)\left(\dot{m}_{\mathrm{V,i}} - \Delta\dot{m}_{\mathrm{L}}\right) \quad (5)$$
$$+ \left(h_{\mathrm{Vsat}} - \Delta h_{\mathrm{LV}} - \overline{\Delta h_{\mathrm{SC,o}}}\right)\left(\dot{m}_{\mathrm{L,i}} + \Delta\dot{m}_{\mathrm{L}}\right)$$

The subtraction from Eq. (5) to Eq. (4) gives the total heat exchange through a segment.

$$\left(h_{\mathrm{b,i}} - h_{\mathrm{b,o}}\right)\dot{m}_{\mathrm{total}}$$
$$= \underbrace{\left(\overline{\Delta h_{\mathrm{SH,i}}} - \overline{\Delta h_{\mathrm{SH,o}}}\right)\dot{m}_{\mathrm{V,i}} + \overline{\Delta h_{\mathrm{SH,o}}}\Delta\dot{m}_{\mathrm{L}}}_{SH} \quad (6)$$
$$+ \underbrace{\Delta h_{\mathrm{LV}}\Delta\dot{m}}_{latent} + \underbrace{\left(\overline{\Delta h_{\mathrm{SC,o}}} - \overline{\Delta h_{\mathrm{SC,i}}}\right)\dot{m}_{\mathrm{L,i}} + \Delta h_{\mathrm{SC,o}}\Delta\dot{m}_{\mathrm{L}}}_{SC}$$

In the right of Eq. (6), the first, second, and third terms shows heat transfer rate caused by de-superheating of vapor flow, latent heat rejection to generate condensate, and subcooling of condensate.

$$\dot{Q}_{\mathrm{total}} = \dot{Q}_{\mathrm{SH}} + \dot{Q}_{\mathrm{latent}} + \dot{Q}_{\mathrm{SC}} \quad (7)$$
$$q_{\mathrm{total}} = q_{\mathrm{SH}} + \left(q_{\mathrm{latent}} + q_{\mathrm{SC}}\right) \quad (8)$$

The driving temperature difference for the heat flux caused by de-superheating q_{SH} is probably the difference from bulk temperature to saturation temperature on the liquid film surface (T_{rb} - T_{sat}). The remaining summation of heat fluxes (q_{latent} + q_{SC}) is manipulated as a heat flux by saturated condensation. Because condensation requires degree of subcool of cooling surface, the HTC of saturated condensation α_{TP} always includes both heat fluxes. That driving temperature difference is normally taken as a difference from saturation temperature to wall temperature (T_{sat} - T_{wi}). Thus, Eq. (9) is converted with those HTCs driving temperature differences to,

$$\alpha\left(T_{\mathrm{rb}} - T_{\mathrm{wi}}\right) = \alpha_{\mathrm{SH}}\left(T_{\mathrm{rb}} - T_{\mathrm{sat}}\right) + \alpha_{\mathrm{TP}}\left(T_{\mathrm{sat}} - T_{\mathrm{wi}}\right) \quad (9)$$

EXPERIMENTAL SETUP AND METHOD

Figure 2 shows the schematic diagram of experimental apparatus. The loop for CO_2 and R410A consists mainly of a variable speed gear pump, a coriolis-type mass flow meter, an electric pre-heater, a mixer, a pre-cooler, a test section, two after-coolers, and receiver tank. In a mixer, placed at entrance of the pre-heater, pressure and bulk-mean temperature of superheated vapor are measured. System pressure is adjusted roughly by refrigerant charge amount and precisely by inlet temperature and flow rate of cooling water flow through the after-coolers.

Test section and test tube

Figure 3 (a) and (b) show a structure of the test section and dimensions of the test tube. The test tube, which is a smooth copper tube of 6.1 mm ID and 9.53 mm OD, is placed horizontally and covered with a thick brass jacket.

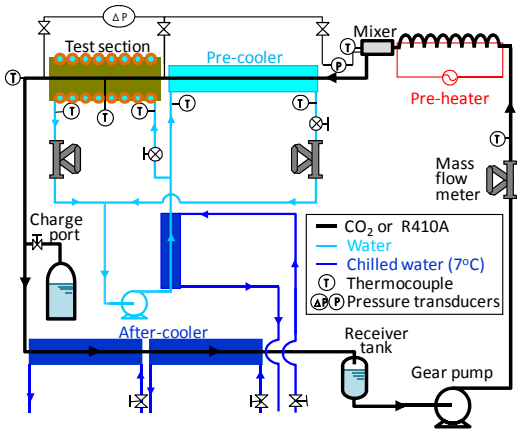

Figure 2 Schematic diagram of the experimental apparatus

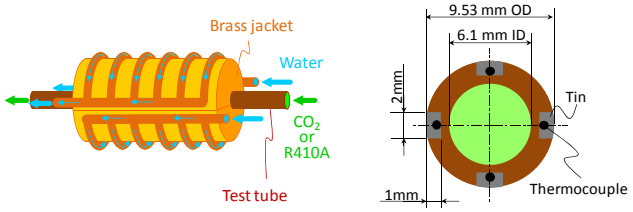

(a) Test section (b) Dimensions of the test tube

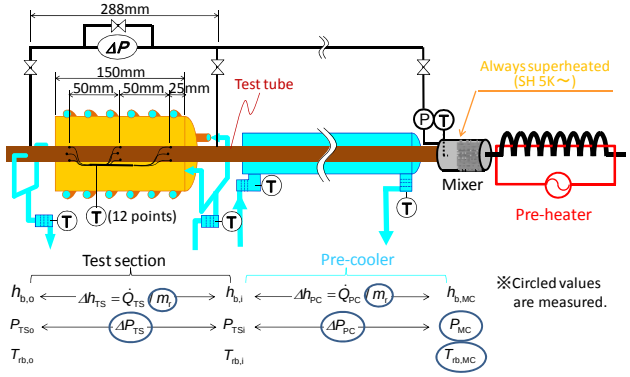

(c) Data reduction procedure

Figure 3 Specifications of the test section and test tube

The halved brass jacket is pressed over the test tube and the small gap between them is filled with a thermal paste. On the outside of the brass jacket, copper tubes are attached with solder allowing cooling water to flow through. This structure yields cooling conditions with an almost uniform temperature. Twelve thermocouples are embedded into the top, bottom, right, and left of the test tube wall at three positions in an axial direction. The active cooling length by the brass jacket is 150 mm, which is relatively short for measuring quasi-local HTC in axial direction.

Experimental Procedure

When measuring heat transfer in superheat zone refrigerant superheat at the test section inlet is controlled from 5 to 40 K by pre-heater; meanwhile, water flow of pre-cooler is shut. During measurements in two-phase zone and superheat zone

below 5 K of superheat, superheated fluid flow through the mixer is kept approximately 5 K for finding bulk enthalpy; meanwhile, inlet condition of the test section is controlled by flow rate and inlet temperature of cooling water flow through the pre-cooler.

Data Reduction Procedure

Figure 3 (c) helps presenting the data reduction method. The main measured values are the refrigerant mass flow rate $\dot{m}_r$, bulk-mean temperature $T_{rb,MC}$, and absolute pressure P_{MC} in the mixer, the bulk water temperature of pre-cooler inlet $T_{H2O,PCi}$ and outlet $T_{H2O,PCo}$, test section inlet $T_{H2O,TSi}$ and outlet $T_{H2O,TSo}$, and the water mass flow rate of pre-cooler $\dot{m}_{H2O,PC}$ and test section $\dot{m}_{H2O,TS}$. The bulk-mean enthalpy in the mixer $h_{rb,MC}$ is obtained from $T_{rb,MC}$ and P_{MC} under the assumption of equilibrium by RefpropVer.8.0 [10]. The enthalpy changes through the pre-cooler Δh_{PC} and the test section Δh_{TS} are determined by water side heat balances and as below.

$$\Delta h_{PC} = \left[\left(T_{H2O,PCo} - T_{H2O,PCi} \right) \dot{m}_{H2O,PC} Cp_{H2O} - \dot{Q}_{gain,PC} \right] \Big/ \dot{m}_r \quad (10)$$

$$\Delta h_{TS} = \left[\left(T_{H2O,TSo} - T_{H2O,TSi} \right) \dot{m}_{H2O,TS} Cp_{H2O} - \dot{Q}_{gain,TS} \right] \Big/ \dot{m}_r \quad (11)$$

where $\dot{Q}_{gain,PC}$ and $\dot{Q}_{gain,TS}$ are preliminarily measured heat leak from ambient air through the insulators. The bulk mean temperature at the test section T_{rb} is obtained from bulk enthalpy and pressure with the equibilium state function of RefpropVer.8.0 [10].

$$T_{rb} = \left(T_{rb,i} + T_{rb,o} \right) \Big/ 2$$

$$T_{rb,i} = f_{equiblium} \left(h_{b,MC} - \Delta h_{PC}, P_{MC} - \Delta P_{PC} \right) \quad (12)$$

$$T_{rb,o} = f_{equiblium} \left(h_{b,MC} - \Delta h_{PC} - \Delta h_{TS}, P_{MC} - \Delta P_{PC} - \Delta P_{TS} \right)$$

The average heat flux of the test section on the interior tube wall q_{wi} is,

$$q_{wi} = \frac{\left(T_{H2O,TSo} - T_{H2O,TSi} \right) \dot{m}_{H2O,TS} Cp_{H2O} - \dot{Q}_{gain,TS} - \dot{Q}_{cond}}{\left(d_i \cdot \pi \cdot \Delta Z_\alpha \right)} \quad (13)$$

where $\dot{Q}_{cond}$ is the conduction heat from outside the cooling brass jacket estimated numerically for each condition. Procedure of numerical analysis and typical results on $\dot{Q}_{cond}$ are specified in Ref. [8]. The definition of average heat transfer coefficient α is,

$$\alpha = \frac{q_{wi}}{\Delta T}, \qquad \Delta T = T_{rb} - T_{wi} \quad (14)$$

where T_{wi} is the averaged temperature of the 12 points on the tube wall. The reference refrigerant temperature is defined as an arithmetic mean of inlet and outlet bulk temperatures $T_{rb,i}$ $T_{rb,o}$, which are found from each pressure P_{TSi} and P_{TSo} and enthalpies $h_{b,i}$ and $h_{b,o}$. With this method, driving temperature difference ΔT in superheat zone is defined as the difference between tube wall and bulk refrigerant temperature. Then this continuously changes into the difference between tube wall and saturation temperature at the thermodynamic vapor quality 1.0 for two-phase zone.

Table 1 lists the measurement uncertainties obtained from the results of two standards deviation of calibration, resolution of data loggers and calibration tools, and the stability of excitation voltages. Combined measured uncertainties are calculated from those uncertainties in conformity of Refs. [11] and [12]

Table 1 Measurement uncertainties

Nomenclature	Instrument	Uncertainty
T_{rb}, T_{H2O}	Sheathed T type Thermocouple	±0.05 K
T_{wi}	Twisted T type Thermocouple	±0.10 K
P_{MC}	Diaphragm absolute pressure transducer	±0.05 MPa
ΔP	Diaphragm differential pressure transducer	±0.26 kPa
$\dot{m}_{H2O,TS}$, $\dot{m}_r$	Coriolis mass flow meter	±0.1 g s^{-1}
$\dot{m}_{H2O,PC}$	Coriolis mass flow meter	±0.5 g s^{-1}

RESULTS AND DISCUSSION

Identification of Condensation from Superheated Vapor

Figure 4 shows experimental results for temperature and derived HTC compared to selected correlations. Figure 4 (a) is R410A at 2.7 MPa, 200 kg $m^{-2}s^{-1}$, and 10 kW m^{-2}, which is the typical condition for A/C condensers in summer season. Figure 4 (b) and (c) are the results of R410A and CO_2 at same reduced pressure P/P_{crit}= 0.81. The horizontal axes show the bulk-mean enthalpy h_b and the top axes in upper graphs show vapor quality x_b. These are obtained from bulk mean temperature of superheated vapor $T_{b,MC}$ under the assumption of equilibrium. The upper graphs show the bulk-mean refrigerant temperature of the test section inlet $T_{rb,i}$ and outlet $T_{rb,o}$, and averaged tube wall temperatures T_{wi}. The center graphs show the representative temperature difference $(T_{rb,i} + T_{rb,o})/2 - T_{wi}$. The bottom graphs show the average HTC α of the test section and five comparative correlations. The bars show measurement uncertainties vertically and enthalpy changes through the test section horizontally.

As shown in Fig. 4 (b), this study specifically categorizes the heat rejection process as superheat, two-phase, and subcool zone where the bulk-mean refrigerant temperature is superheated, saturated, and subcooled, respectively. The dashed lines in Fig. 4 are selected correlations of Gnielinski [13] with Petukov's correction factor [14] for superheat zone, Cavallini [15] for two-phase zone, and Gnielinski [13] with Sieder-Tate's correction factor [16] for subcool zone.

As shown in Fig. 4 (a), experimental HTC starts gradually increasing from Gnielinski's correlation when the average temperature of tube wall T_{wi} reaches saturation point. This start point strongly supports the identification of condensation in presence superheated vapor. Thus, the superheat zone could be subdivided into single-phase superheat zone (I) and condensing superheat zone (II) by condensation occurrence.

Modification of the Saturated Condensation Correlation near Critical Point

Figure 5 (a) shows the change of experimental and predicted HTC of CO_2 condensation/cooling across the critical point 7.4 MPa, and 344 kJ kg^{-1}. Figure 5 (b) is HTC of R410A across the critical point 4.9 MPa, and 368 kJ kg^{-1}. As shown with dashed line in Fig. 5 and other experimental data, predicted HTC by Cavallini's correlation [15] shows excellent agreement with our data. Nevertheless, it deviates from our data at high reduced pressure (0.8 to 1) – not surprisingly because that range was not included in original correlation. To correct Cavalini's correlation at these high reduced pressures we found background in Fujii et al. [17], [18] who theoretically verified extension of Nesselt's filmwise condensation theory [19] up to reduced pressure 0.995 by using liquid properties at the film temperature.

Figure 6 shows the calculation results of CO_2 specific heat from the tube wall to liquid surface, where almost saturation condition, at the 6, 7 and 7.36 MPa, and temperature difference 5 K. Temperature distribution in the liquid film is assumed linear. Near the critical pressure at 7.36 MPa, specific heat drastically increases towards the liquid surface. Similarly, thermal conductivity and Prandtl number increase while viscosity and density decrease. Therefore selection of characteristic temperature for liquid properties becomes even more important near the critical point. Equation 5 is our modification of Cavallini's correlation with $\overline{Cp}_L$, as shown in Fig. 6, and film temperature.

$$J_G = x_b G_r \Big/ \sqrt{g d_i \rho_{Vsat} \left(\rho_{Lsat} - \rho_{Vsat}\right)}$$

$$J_G{}^T = \left\{ \left(7.5/4.3 X_{tt}{}^{1.111} + 1\right)^{-3} + 2.6^{-3} \right\}^{-1/3}$$

$$\alpha_{LO\_f} = 0.023 \left(G_r d_i / \mu_{L\_f}\right)^{0.8} Pr_{L\_f}{}^{0.4} \left(\lambda_{Lsat} / d_i\right)$$

$$Pr_{L\_f} = \left(\overline{Cp}_L \mu_{L\_f}\right) \Big/ \lambda_{L\_f}$$

$$\overline{Cp}_L = \left(h_{Lsat} - h_{L,wi}\right) \Big/ \left(T_{sat} - T_{wi}\right)$$

$$\alpha_{strat} = 0.725 \left[\frac{\lambda_{L\_f}{}^3 \rho_{L\_f} \left(\rho_{L\_f} - \rho_{Vsat}\right) g \Delta h_{LV}}{\mu_{L\_f} d_i \left(T_{sat} - T_{wi}\right)} \right]^{0.25} \times \left\{ 1 + 0.741 \left(\frac{1 - x_b}{x_b} \right)^{0.3321} \right\}^{-1} + \left(1 - x_b{}^{0.087}\right) \alpha_{LO\_f}$$

$$\alpha_{TP} = \begin{cases} J_G > J_G{}^T : \\ \alpha_A = \alpha_{LO\_f} \left[1 + 1.128 x_b{}^{0.8170} \left(\rho_{Lsat} / \rho_{Vsat}\right)^{0.3685} \right. \\ \left. \left(\mu_{Lsat} / \mu_{Vsat}\right)^{0.2363} \left(1 - \mu_{Vsat} / \mu_{Lsat}\right)^{2.144} Pr_{L\_f}{}^{-0.1} \right] \\ \\ J_G \le J_G{}^T : \\ \left[\alpha_A \left(J_G{}^T / J_G\right)^{0.8} - \alpha_{strat} \right] \left(J_G / J_G{}^T\right) + \alpha_{strat} \end{cases} \quad (15)$$

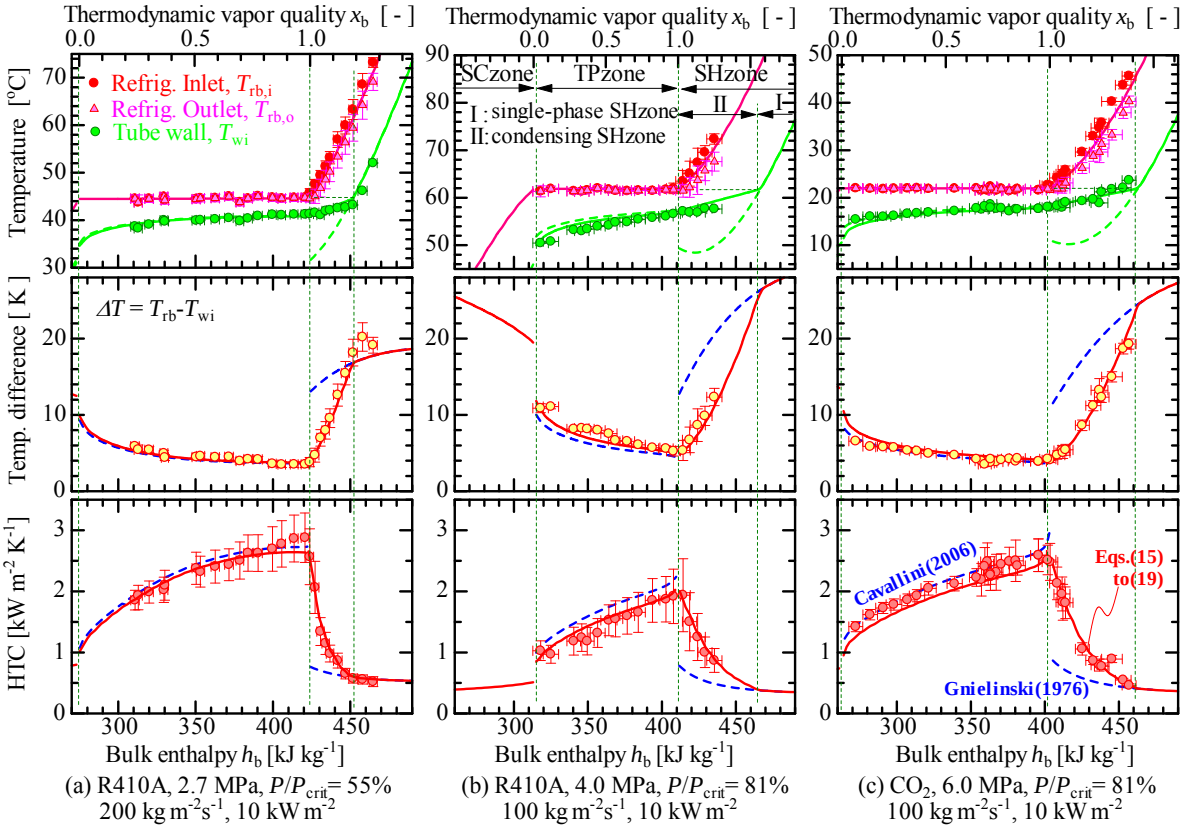

Figure 4 Comparison between experimental results and predictions for HTC: Dashed lines --- Cavallini [15] and Gnielinski [13], Solid lines — Eqs. (15) to (19).

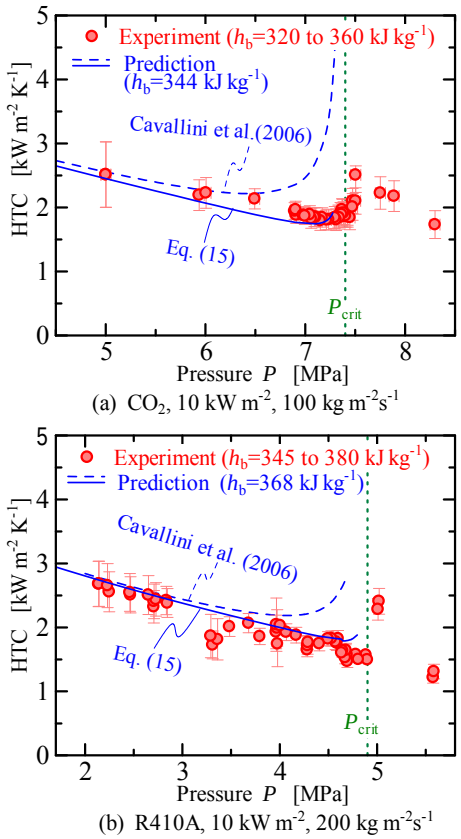

Figure 5 Changes of HTC towards the critical points

where, subscript "_f" indicates the value evaluated at the film temperature which is the modified value from the original. As shown with solid line in Figs. 5 (a) and (b), this modified correlation satisfactorily agrees with experimental HTC until reduced pressure 0.975 for CO_2 and R410A both.

Proposal of a Prediction Method for Condensing SH Zone

From Eq. (10), HTC in condensing superheat zone is expressed as,

$$\alpha_{total} = \left[\alpha_{SH}\left(T_b - T_{sat}\right) + \alpha_{TP}\left(T_{sat} - T_{wi}\right)\right] \Big/ \left(T_b - T_{wi}\right) \quad (16)$$

Here, α_{TP} is calculated by modified Cavallini's correlation Eq. (15). However, the assumption of same flow regime as vapor quality 1.0 is required for solving the equation. As a computational procedure, Martinelli parameter X_{tt}, dimensionless gas velocity J_G and $J_G{}^T$, and fully-stratified HTC α_{strat}, were calculated same as when vapor quality at 0.995. In the correct way, the correlation should be newly developed with actual vapor mass quality accounting non-equilibrium condition. However, this concept requires multiple iterations and might not worth for the calculation for only superheat zone. In order to avoid further computational load and iteration errors, this paper recommends above supplement method with existing correlations. Next, α_{SH} is calculated by the correlation Gnielinski [13] with Petukov's correction factor F_a [14] as below.

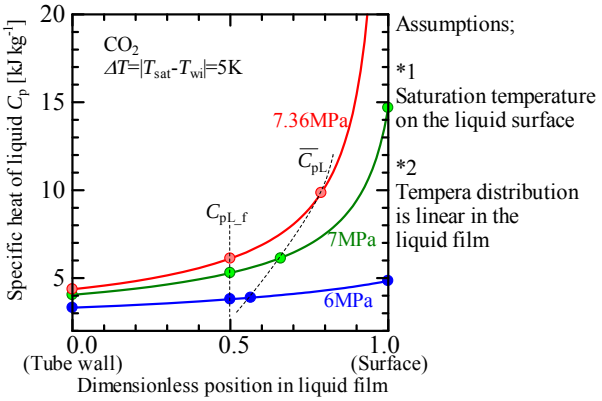

Figure 6 Example of specific heat distribution in liquid film.

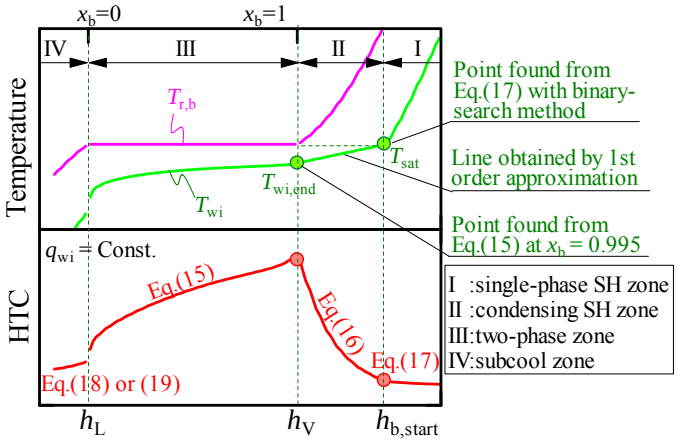

Figure 7 Overview of calculation procedure

$$\alpha_{SH} = Nu_0 F_a\left(\lambda_b/d_i\right), \quad F_a = \left(T_{wi}/T_{rb}\right)^{-0.36}$$
$$Nu_0 = \frac{\left(f_b/8\right)\left(G_r d_i/\mu_b - 1000\right)Pr_b}{1 + 12.7\left(f_b/8\right)^{1/2}\left(Pr_b^{2/3} - 1\right)} \quad (17)$$
$$f_b = \left[1.82 \cdot \log_{10}\left(G_r d_i/\mu_b\right) - 1.64\right]^{-2}$$

where f_b is Filonenko's friction factor [20].

Calculation Procedure from Superheat Zone to Subcool Zone

Figure 7 shows the overview of calculation procedure. The start point of condensation $h_{b,start}$ was found by binary search method with the criterion T_{wi} = T_{sat} and Eq. (17). At vapor quality 1.0, the tube wall temperature $T_{wi,end}$ is found by Eq. (15). The line connects two points ($h_{b,start}$, T_{sat}) and (h_V, $T_{wi,end}$) is obtained from first order approximation. As shown with green solid lines of upper graphs in Fig. 4, this approximation satisfactorily agrees with experimental data and allows reducing one loop of iteration. HTC in subcool zone α_{SC} is predicted by Gnielinski [13] with Sieder and Tate's correction factor F_a [16] as below.

$$\alpha_{SC} = Nu_0 F_a\left(\lambda_b/d_i\right), \quad F_a = \left(\mu_b/\mu_{wi}\right)^{0.14} \quad (18)$$

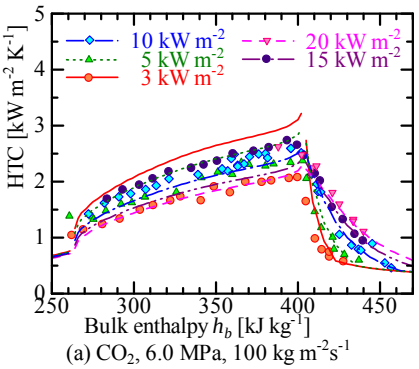

(a) CO_2, 6.0 MPa, 100 kg m^{-2}s^{-1}

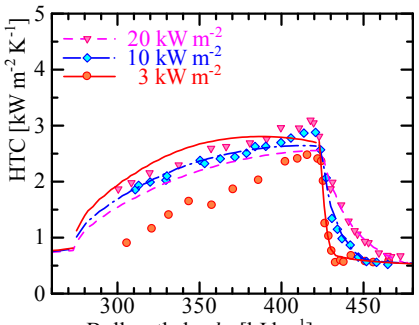

(b) R410A, 2.7 MPa, 200 kg m^{-2}s^{-1}

Figure 8 Experimental HTC of various heat fluxes and proposed correlations.

When reduced pressure P/P_{crit} is above 0.9 and refrigerant mass flux G_r is above 150 kg m^{-2}s^{-1}, Eq. (18) gives higher HTC than experimental HTC and Eq. (15) at vapor quality 0. The radial properties change becomes too drastic to be corrected by Sieder and Tate's factor. For better interrelating between two-phase zone and subcool zone, below correlation using Pr_{L_f} is better to applied.

$$P/P_{crit} > 0.9 \text{ and } G_r > 150 \text{ kg m}^{-2}\text{s}^{-1}:$$

$$\alpha_{SC} = Nu_f \left(\lambda_{L\_f}/d_i\right)$$

$$Nu_f = \frac{\left(f_f/8\right)\left(G_r d_i/\mu_{L\_f} - 1000\right)Pr_{L\_f}}{1 + 12.7\left(f_f/8\right)^{1/2}\left(Pr_{L\_f}{}^{2/3} - 1\right)} \qquad (19)$$

$$f_f = \left[1.82 \cdot \log_{10}\left(G_r d_i/\mu_{L\_f}\right) - 1.64\right]^{-2}$$

Comparison between Calculation and Experimental Results

Predicted temperatures and HTC are shown with blue solid lines in Fig. 4. As the comparison, above calculation results satisfactorily agree with experimental results of R410A and CO_2 both. The remarkable improvement is the tube wall temperature of the zone, where condensation occurs in superheated vapor. The correlation, which does not account condensation, gives over 10 K lower tube wall temperature near vapor quality 1.0 and it is not negligible deviation for circuit design of condensers. Compared with this, the newly proposed calculation method predicts the temperature with accuracy within 2 K approximately.

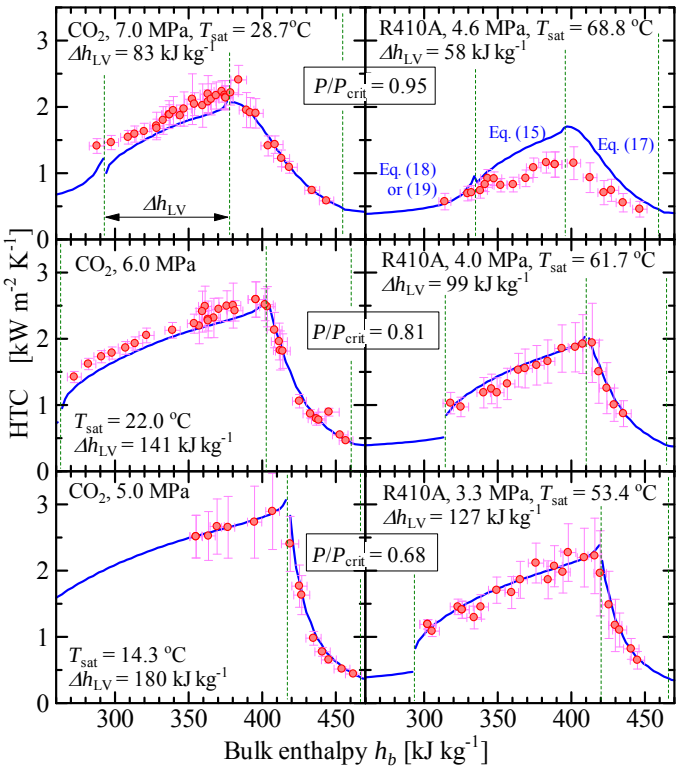

Figure 9 Comparison on HTC between CO_2 and R410A at the same reduced pressure.

Figure 8 shows comparison of the experimental HTC of various heat fluxes to the correlations Eqs. (15) to (19) effect of heat flux on the start point of condensation. Since tube wall temperature tends to be lower at higher heat flux, the temperature reaches saturation point earlier and condensation starts earlier with increasing heat flux. This tendency is predicted by the proposed correlations and the curve of calculation results overlaps experimental data point satisfactorily in the zone of condensation of superheated vapor.

Comparison of HTC between CO_2 and R410A at the Same Reduced Pressure

Figure 9 shows HTC of CO_2 in the three left graphs and R410A in the right graphs at 100 kg m^{-2}s^{-1}, 10 kW m^{-2}, and reduced pressures P / P_{crit} 0.68, 0.81 and 0.95. Each saturation temperature T_{sat} and latent heat Δh_{LV} is shown with the conditions in those graphs. Vertical green dashed line divides zones into single-phase superheat, condensing superheat, two-phase, and subcool from right to left. Red symbols shows experimental HTC blue solid lines are calculated HTC by Eqs. (15) to (19) for superheat and two-phase zones.

In single-phase superheat zone, HTC of CO_2 is barely higher than R410A at the same reduced pressure. In two-phase zone, HTC of CO_2 exceeds R410A. HTC almost always has maximum at the border between two-phase and superheat zone (x_b = 1).The maximum HTC of CO_2 is roughly 120 to 170 % of R410A at the reduced pressure from 0.68 to 0.95. As Nusselt's film wise condensation theory describes, latent heat Δh_{LV} is the most dominant parameter on condensation HTC. Larger latent

heat means that released heat from a mass of vapor is larger at the moment of phase change and increases condensation HTC. As noted in the graphs, the latent heat of CO_2 is roughly 140% of R410A and this increases HTC in two-phase zone.

Although experimental HTC and calculated HTC satisfactorily agree in general, experimental HTC of R410A slightly deviates when approaching critical point and is approximately 25% below from correlation at reduced pressure 0.95.

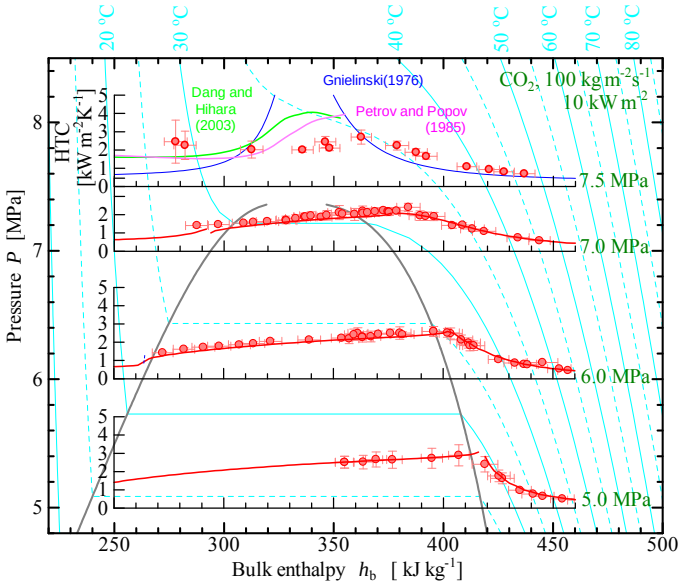

(a) CO_2 at 100 kg m^{-2} s^{-1}, 10 kW m^{-2}

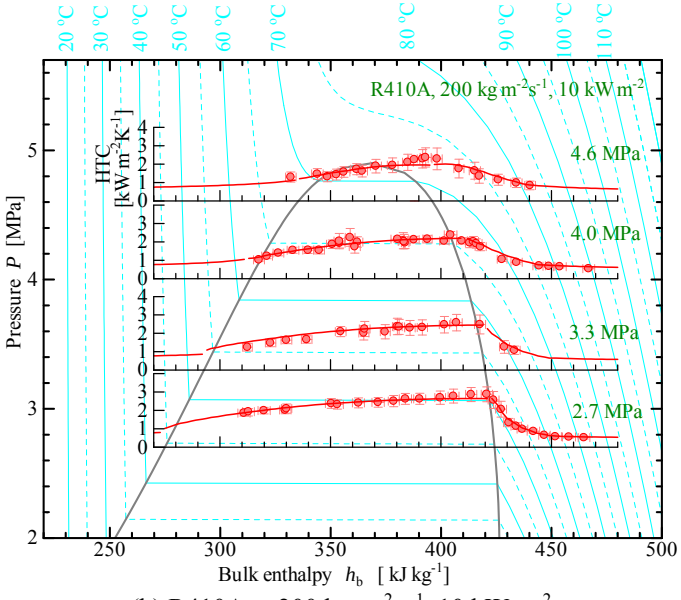

(b) R410A at 200 kg m^{-2} s^{-1}, 10 kW m^{-2}

Figure 10 Summary of experimental HTC and correlation. (Symbol – experiment, Red lines –newly proposed correlations Eqs. (15) to (19), blue pink, green lines are correlations by Gnieslineki (13), Petrov [21], and Dang [22] respectively)

Summary of Experimental Results and Correlations through the Superheat, Two-Phase, and Subcool Zone

Figure 10 shows experimental and predicted HTC of various pressures of CO_2 and R410A. In Fig. 10, symbols show experimental HTC and red lines show the newly proposed correlation Eqs. (15) to (19). The predicted HTC by newly proposed correlation agrees with experimental HTC for both refrigerant and condition.

Figure 10 purposely plots HTC data on the *P-h* diagram for better for better understanding of the portion of condensing superheat zone in entire enthalpy change through a condenser inlet to outlet. For instance, when a condenser inlet to outlet temperature of R410A system is 90°C to 45°C at 2.7 MPa, the enthalpy change in condensing superheat zone is approximately 14%. At 4.6 MPa, the enthalpy change is approximately 21%. Likewise, the enthalpy change ratio of condensing superheat zone to the entire zone becomes larger and important for condenser design.

Similarity between Supercritical and Subcritical Heat Rejection process

Figure 10 (a) includes some HTC data of CO_2 at 7.5 MPa, just above the critical pressure. In the graph of CO_2 at 7.5 MPa, blue, pink, and green lines show correlations by Gnielinski [13], Petrov and Popov [21], Dang and Hihara [21]. Gnielinski correlation, which is valid at subcritical pressure, shows higher HTC than experimental data especially around the pseudo-critical point 350 kJ kg^{-1}. This is due to the drastic property change in radial direction. Other two correlations by Petrov and Popov [21], Dang and Hihara [21] take into consideration the strong radial property change. Hence the maximum HTC of Petrov and Popov's and Dang and Hihara's correlations are much closer to the experimental HTC.

There are liquid and gas (not to be called vapor) even above the critical pressure. Liquid and gas coexist as fluctuating spatially and temporally. The pseudo-critical point shows the border of both phases. Near the critical point, the gas still needs to release much energy when it changes into liquid as if vapor releases latent heat. Thus, a similar phenomenon to superheat zone condensation occurs in the supercritical heat rejection process when the pseudo-critical temperature is sandwiched between the bulk and wall temperatures.

For instance, the experimental HTC is 2.5 kW m^{-2} K^{-1} and the bulk refrigerant temperature is 31.8 °C around the pseudo-critical point of 350 kJ kg^{-1}. The temperature difference is 4 K, the tube wall temperature is 27.8°C, and the refrigerant enthalpy at 27°C is 278 kJ kg^{-1}. This means the enthalpy is radially distributed from 350 to 278 kJ kg^{-1}. This large enthalpy change is comparable to latent heat, and the HTC should be determined by the thermal properties of this averaged value. Therefore, it is not surprising that experimental HTC shows much more moderate peak than Gnielinski correlation.

Furthermore, the supercritical HTC has the maximum point above the pseudo-critical temperature (enthalpy) for the similar reason of superheat zone condensation. The tube wall reaches a pseudo-critical point ahead of core flow in the center of tube. Goldman (1961), Tanaka et al. (1968) and Yamagata et al. (1972) have confirmed same peak shift and that the maximum

HTC appears just above the pseudo-critical temperature under cooling conditions and just below it under heating conditions.

CONCLUSION

Experimental results for heat rejection from CO_2 and R410A near the critical points have been provided. The predicting correlation has developed for condensing superheat zone. The results have been compared to existing correlations and newly developed correlation. The main findings are following:

- Heat rejection process is categorized as superheat, two-phase, and subcool zone by bulk mean temperature. Further, the superheat zone can be subdivided into single-phase superheat zone and condensing superheat zone based on condensation occurrence.

- Condensation starts in presence of superheated vapor when tube wall temperature reaches saturation temperature. This is demonstrated by experimental HTC, which gradually starts increasing from Gnielinski correlation exactly at that point tube wall reaches saturation temperature.

- At the same reduced pressure 0.81, HTC of CO_2 is significantly higher than R410A in two-phase zone. The main reason appears to be the larger latent heat of CO_2 than R410A.

- Modified Cavallini's correlation, which evaluates liquid properties at the film temperature, well predicts HTC at reduced pressure up to 0.975.

- Newly developed correlation, which complements between Gnielinski's and Cavallini's correlation, has been proposed for condensing superheat zone. This correlation satisfactorily agrees with the experimental results in the range of this experiment.

- Above the critical pressure, the maximum value of experimental HTC is much lower than Gnielinski's correlation due to strong property change in radius direction. The value is closer to Petrov and Popov, and Dang and Hihara's correlations accounting for the radial property changes.

- Above the critical pressure, experimental HTC shows maximum value above the pseudo-critical temperature, because, tube wall reaches a pseudo-critical point ahead of core flow similar to condensing superheat zone.

REFERENCES

[1] Balekjian, G., Katz, D., Heat transfer from superheated vapors to a horizontal tube, *A.I.Ch.E. J.*, 4 (1) 1958, pp. 43-48.

[2] Altman, M., Staub, F.W., Norris, R.H., Local heat transfer and pressure drop for refrigerant-22 condensing in horizontal tubes, *Chem. Eng. Progress symposium series*. 56 (30) 1959, pp. 151-159.

[3] Bell, K.J., Temperature profiles in condensers, *Chem. Eng. Prog.*, 68 (7) 1972, pp. 81-82.

[4] Miropolsky, Z.L., Shneersva, R.I., Teernakova, L.M., Heat transfer at superheated steam condensation inside tubes, *Proc. 5th Int. Heat Trans. Conf.*, Vol. 3, September 3-7, Tokyo, Japan, 1974 , pp. 246-249.

[5] Fujii, T., Honda, H., Nozu, S., Nakarai, S., Condensation of superheated vapor inside a horizontal tube, *Heat Transfer - Japanese Research*, 4 (3), 1978, pp. 1-48.

[6] Lee, C.C., Teng, Y.J., Lu, D.C., Investigation of condensation heat transfer of superheated R-22 vapor in a horizontal tube, *Proc. World Conf. Exp. Heat Trans. Fluid Mech. and Thermodynamics.*, in: J.F. Keffer, R.K. Shah, E.N. Ganić (Eds.) 1991, pp. 1051-1057.

[7] Webb, R.L., Convective condensation of superheated vapor, *Trans. ASME, J. Heat transfer*, 120, 1998, pp. 418-421.

[8] Kondou, C., Hrnjak, P.S., Heat rejection from R744 flow under uniform temperature cooling in a horizontal smooth tube around the critical point, *Int. J. Refrig.*, 34 (3) 2011, pp. 719-731.

[9] Soliman, H.M., The mist-annular transition during condensation and its influence of the heat transfer mechanism, *Int. J. Multiphase Flow*, 12 (2) 1986, pp. 277-288.

[10] Lemmon, E.W., Huber, M.L., McLinden, M.O., Reference fluid thermodynamic and transport properties - REFPROP ver. 8.0, NIST, Boulder, CO, 2007.

[11] ASME Performance Test Codes, Supplement on Instrument and Apparatus, Part1, *ASNSI / ASME PTC*, 1985, 19.1-1985.

[12] Moffat, R.J., Description uncertainties in experimental results, *Exp. Therm. Fluid Sci.*, 1, 1988, pp. 3-17.

[13] Gnielinski, V., New equation of heat and mass transfer in turbulent pipe and channel flow, *Int. Chem. Eng.*, 16, 1976, pp. 359-367.

[14] Petukhov, B.S., Heat transfer and friction in turbulent pipe flow with variable physical properties, *Advances Heat Transf.*, 6, Academic Press, Orland, 1970, pp. 503-564.

[15] Cavallini, A., Del Col, D., Doretti, L., Matkovic, M., Rossetto, L., Zilio, C., and Censi, G., Condensation in horizontal smooth tubes: a new heat transfer model for heat exchanger design, *Heat Trans. Eng.*, 27 (8) 2006, pp. 31-38.

[16] Sieder, E.N. and Tate, G.E., Heat transfer and pressure drop of liquids in tubes, *Ind. Eng. Chem.*, 28, 1936, pp. 1429-1435.

[17] Fujii, T., Lee, J.B., Shinzato, K., Laminar forced convection of saturated vapors in the near-critical region, *Int. J. Numer. Heat Transfer*, Part A, Vol. 30, 1996, pp. 799-813.

[18] Fujii, T., Lee, J.B., Shinzato, K., Makishi, O., Laminar free convection condensation of saturated vapors in the near-critical region, *Int. J. Numer. Heat Transfer*, Part A, Vol. 31, 1997, pp. 373-385.

[19] Nusselt, W., Die Oberflachenkondensation des wasserdampfes, Vereines Deutscher Ingenieure, Vol. 60, No. 27, 1916, pp. 541-546. (in German)

[20] Filonenko, G. K., Hydraulic drag in pipes, *Teploenergetika*, 1 No. 4, 1954, pp. 40-44 (in Russian)

[21] Petrov, N.E., Popov, V.N., 1985. Heat transfer and resistance of carbon dioxide being cooled in the supercritical region, *Thermal Eng.*, 32 (3), 1985, pp. 131-134.

[22] Dang, C., Hihara, E., Cooling heat transfer of supercritical carbon dioxide: A new correlation for heat transfer coefficient and effect of lubricant oil, *Trans. JSRAE*, 120, (2) 2003, pp. 175-183 (in Japanese).

[23] Goldman, K., Heat transfer to supercritical water at 5000 psi flowing at high mass flow rate through round tubes, A*SME Int. Dev. in Heat Transfer*, Part III, 1961, pp. 561-568.

[24] Tanaka, H., Nishikawa, N., Hirata, M., Turbulent heat transfer to supercritical carbon dioxide, *Proc. 1967 Semi-Int. symp. Heat Mass Transfer*, Vol.2 1968, pp. 127-134.

[25] Yamagata, K., Nishikawa, K., Hasegawa, S., Fujii, T., Yoshida, S., Forced convective heat transfer to supercritical water flowing in tubes, *Int. J. Heat Mass Transfer*, 15, 1972, pp. 2575-2593.